*Progress In Electromagnetics Research C, Vol. 55, 149–157, 2014*

# A Compact UWB Printed Antenna with Bandwidth Enhancement for In-Body Microwave Imaging Applications

**Aref Abdollahvand[1, *], Abbas Pirhadi[2], Homauon Ebrahimian[3], and Mousa Abdollahvand[4]**

**Abstract**—In this paper, we propose novel omnidirectional UWB printed monopole antenna for in-body microwave imaging applications. The proposed antenna consists of a square radiating patch, a microstrip feed line and a ground plane with two resonant elements, a pair of rotated T-shaped slots and another T-shaped slot placed in the middle of the pair slots. The designed antenna provides a wide usable fractional bandwidth of more than 136.5% (2.96–15.8 GHz). This antenna has the advantages of wide bandwidth, compact size, low cost, good omnidirectional radiation patterns, and acceptable time domain behavior for using in In-Body microwave applications. The maximum measured gain for the fabricated antenna is around 6.1 dBi with an average efficiency above 89% throughout the bandwidth.

## 1. INTRODUCTION

One of the wireless communication systems that recently has attracted more interest is WBAN systems.

Wireless body area networks (WBANs) can be used for monitoring and communication in diverse application areas such as health care, public safety and defense [1–4]. In general, WBAN systems can be classified into two parts: wearable and implantable systems. Wearable systems are placed on human body and implantable systems are implanted into the human body tissues. In general, wearable systems can be divided into three parts: on-body, in-body, and off-body communications links. In this paper we focuse on in-body wearable systems. These types of WBAN systems have many sensors placed on the human body for propagation into the human body for microwave imaging applications. Microwave imagine systems are used in applications such as tumor detection [5], breast cancer detection [6], brain stroke detections [7], and monitoring of water accumulation in the body [8].

X-RAY mammography is the most common detection technique used in microwave imaging applications.

However, this method has disadvantages such as relatively high missed- and false-detection rates, ionizing radiation, demanding uncomfortable compression of the breast during the examination [9, 10]. In contrast, UWB signal does not ionize and can penetrate human tissues very effectively [11]. Antennas are essential elements wherever wireless communication systems are required. The design of a compact antenna with wide impedance bandwidth and high-performance properties is a significant challenge in microwave imaging applications. A glimpse into the recently designed UWB planar monopole antennas shows that these types of antennas have many advantages that make them a suitable choice in the WBAN systems. UWB technology permits to realize low complexity systems with compact antennas and wide bandwidth results high resolution images.

In general, microwave imaging system is formed by two specific array configurations: planar array and circular cylindrical array. In this paper, we focus on circular cylindrical microwave imaging

*Received 14 November 2014, Accepted 26 December 2014, Scheduled 30 December 2014*

* Corresponding author: Aref Abdollahvand (aref.abdollahvand@gmail.com).
[1] Department of Electrical Engineering, Parsabad Moghan Branch, Islamic Azad University, Parsabad, Iran. [2] Department of Electrical Engineering, Shahid Beheshti University G.C (SBU), Tehran, Iran. [3] Department of Biomedical Engineering, Ardabil Branch, Islamic Azad University, Ardabil, Iran. [4] Department of Electrical and Computer Engineering, Tarbiat Modares University, Tehran, Iran.

technique. In this configuration the patient placed in the prone position and the breast surrounded by a circular array of antennas. Antennas with wide bandwidth, sufficient and moderate gain, omnidirectional radiation patterns and compact size are the principal requirements for antennas in circular cylindrical microwave imaging systems [12, 13].

Recently, various types of UWB antennas for microwave imaging systems have been designed. Planar tapered slot antennas for ultra wideband biomedical microwave imaging system were proposed in [14, 15]. A balanced antipodal Vivaldi antenna with dielectric director for near-field microwave imaging was proposed in [16]. In [17] a diamond shaped small planar UWB antenna for microwave imaging purpose was presented. A double-layer bowtie antenna for medical diagnosis was proposed in [18]. A dielectric-filled slot line bowtie antenna for breast cancer detection was proposed in [19]. A microstrip patch antenna design for breast cancer tumor detection was proposed in [20]. However, each of them has its own merits and drawbacks. Most of these antennas have a significant size, thus difficult for the use as a base for an antenna array. Some of these antennas have low gain or low radiation efficiency, and others have a low bandwidth and do not cover UWB band entirely.

In this paper, we present a novel design of an UWB printed monopole antenna for the use in cylindrical microwave imaging systems. One of the main goals in the proposed structure is to find a planar shape that yields a higher bandwidth. We propose a suitable antenna with wide bandwidth, small size, moderate gain, high efficiency, and suitable time domain behavior for using in microwave imagine applications. The simulated result of the proposed antenna is validated by fabricating a number of antennas and measuring their return loss as well as radiation characteristics.

## 2. ANTENNA CONFIGURATION AND DESIGN

Figure 1 shows the top, bottom and side views of the proposed antenna. The design of the proposed antenna starts by choosing the dimensions of the designed antenna. This antenna is printed on an FR4 microwave substrate with a size of $12 \times 18\,\text{mm}^2$, thickness of 0.8 mm, and relative dielectric constant of 4.4. The proposed antenna consists of a square radiating patch and a ground plane fed by a microstrip line. The patch is connected to a microstrip feed-line with the width of $W_f$ and length of $L_f$. In the microstrip feed line, the impedance of the microstrip line is given by [21]

$$Z_c = \frac{120\pi}{\sqrt{\varepsilon_{reff}}\left[\frac{W_f}{h} + 1.393 + 0.667\ln\left(\frac{W_f}{h} + 1.444\right)\right]}$$

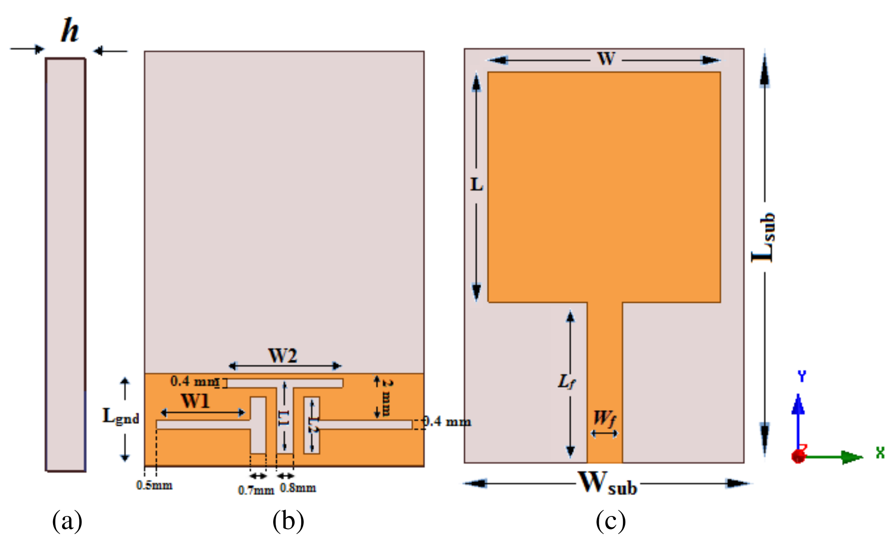


**Figure 1.** The configuration of the proposed, (a) side view, (b) top layer, and (c) bottom layer.

where $W_f$ is the width of the microstrip feed line, $h$ the height of the substrate, and $\varepsilon_{reff}$ the effective dielectric constant and given by $\varepsilon_{reff} = (\varepsilon_r + 1)/2$. So we can calculate the width of the feed line for $Z_c = 50\,\Omega$. In order to have a microstrip feed line with characteristic impedance of $50\,\Omega$, the width $W_f$ of the microstrip feed-line is fixed at 1.5 mm [22]. In the next step, we determine the width and length of the radiating patch. For an efficient radiator, the starting value of $W$ and $L$ are

$$W = \frac{\nu_0}{2f_{\text{center}}}\sqrt{\frac{2}{\varepsilon_r + 1}}, \quad L = \lambda_{\text{lower}}/4$$

where $\lambda_{\text{lower}}$ is the lower bandwidth frequency wavelength. The width of the radiating patch mostly affects the antenna bandwidth. As this parameter increases, so does the antenna bandwidth and vice versa.

$\lambda_{\text{lower}}$ depends on the radiating patch width, thickness and dielectric constant of the substrate. On the other side of the substrate, a conducting ground plane of width $W_{sub}$ and length $L_{gnd}$ is placed. The optimal dimensions of the designed antenna are presented in Table 1.

**Table 1.** Optimal dimensions of the proposed antenna.

| **Parameter** | $mm$ | **Parameter** | $mm$ | **Parameter** | $mm$ |
|---|---|---|---|---|---|
| $W_{sub}$ | 12 | $W$ | 10 | $W_1$ | 4 |
| $L_{sub}$ | 18 | $L$ | 10 | $W_2$ | 5 |
| $h$ | 0.8 | $W_f$ | 1.5 | $L_1$ | 3.3 |
| $L_{gnd}$ | 4 | $L_f$ | 7 | $L_2$ | 2.5 |

In the design of the proposed structure, to create impedance matching that results in bandwidth enhancement, we embedded a pair of rotated T-shaped slots and another T-shaped slot placed in the middle of the pair slots in the ground plane. Figure 2 shows the step by step development of the antenna used for multi-resonance performance simulation.

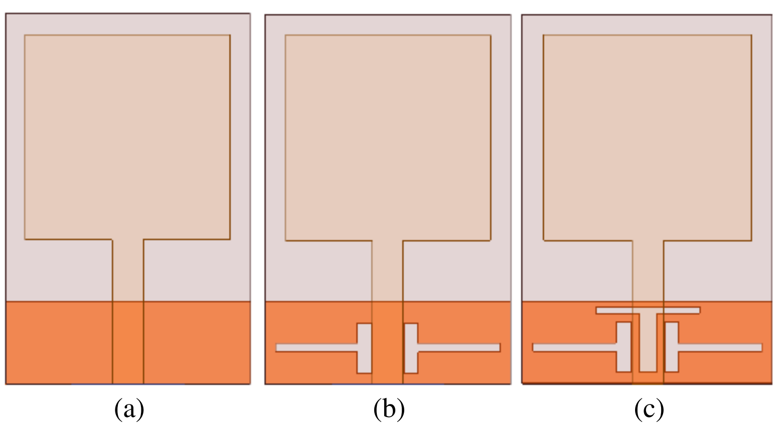


**Figure 2.** The step by step development of the antenna used for multi resonance performance simulation.

## 3. RESULTS AND DISCUSSIONS

This section explains the design steps for the proposed monopole antenna. The proposed antenna was designed using Ansoft HFSS$^{\text{TM}}$ [23] to study in frequency domain and CST MWS [24] to study in time domain. In general, the time domain analysis can be best for wideband antennas and the frequency domain analysis more suitable for electrically small antennas.

### 3.1. Frequency Domain Behavior

In this section, to achieve multi-resonance performance and increase the bandwidth of the proposed structure, a pair of rotated T-shaped slots and another T-shaped slot placed in the middle of the pair slots in the ground plane are adopted. Each slot acts as a resonator at its resonance frequency. Resonant slot length, which is a multiple of quarter-wavelength, can be calculated approximately by $L_{\text{total}} \cong n\lambda_g/4$. For a desired resonant frequency, the wavelength is given by $\lambda_g = \lambda/\sqrt{\varepsilon_{reff}}$, in which $\lambda$ is the free space wavelength and $\varepsilon_{reff}$ the effective permittivity given by a approximate formula of $\varepsilon_{reff} \cong (\varepsilon_r + 1)/2$ [25]. Figure 3 shows the simulated VSWR of various structures shown in Figure 2. Figure 3 shows that an ordinary monopole antenna without proposed slots [structure in Figure 2(a)] has two resonance frequencies in 5 GHz and 9.5 GHz. It is observed that by embedding a pair of rotated T-shaped slots on the ground plane [structure in Figure 2(b)], a new resonance frequency is produced in frequency of 13.4 GHz. In this case, $L_{\text{resonance1}} \cong W_1 + L_2 \cong 2\lambda_g/4$, and $\lambda_g$ is the guided wavelength in the resonance frequency of 13.4 GHz. Also by using a T-shaped slot [structure in Figure 2(c)], the next resonance frequency is excited in frequency of 15.3 GHz, and also the lower frequency bandwidth is affected by using this slot. Indeed, because of electromagnetic coupling (EC) between the first and second resonators, inductance and capacitance of the input impedance are altered and then the lower frequency of the proposed antenna improved. Also, by using this slot, previous resonance frequency in 13.4 GHz is moved to 12.1 GHz. The length of resonator in this frequency is $L_{\text{resonance2}} \cong W_2 + L_1 \cong 3\lambda_g/4$, and $\lambda_g$ is the guided wavelength in the resonance frequency of 15.3 GHz. From Figure 3, we can see that the antenna has a bandwidth ranging from 2.96 to 15.8 GHz for VSWR $< 2$ dB, which is very attractive for UWB microwave imagine application.

The designed antenna was manufactured and tested. Figure 4 shows the measured and simulated VSWRs of the proposed monopole antenna. A good agreement between the simulated and measured results can be observed. However, there is some discrepancy between simulated and measured results due to fabrication tolerance and effect of the connectors.

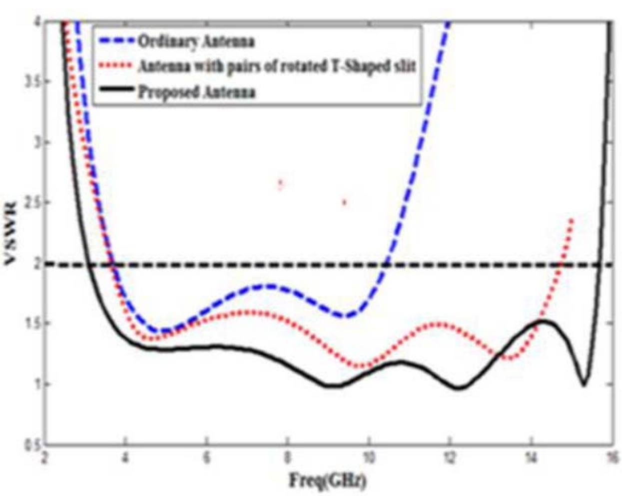


**Figure 3.** Simulated VSWR characteristics of the various structures shown in Figure 2.

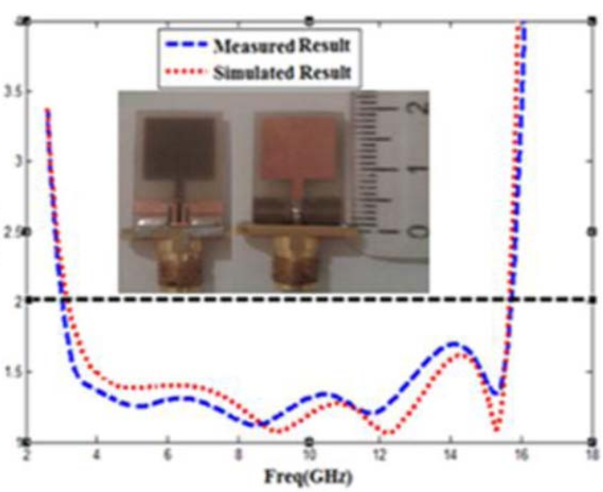


**Figure 4.** Measured and simulated VSWR of the antenna.

Figure 5 presents the simulated and measured peak antenna gains versus frequency. The figure shows that the proposed monopole antenna has relatively flat and constant (variations below 2.5 dB) gain which increases by the frequency. It is observed that the measured gain varies from 3.6 dBi to 6.1 dBi within the band. Thus, the antenna exhibits stable and acceptable gain level across the operation band. Radiation efficiency of the proposed antenna is shown in Figure 6. As can be seen from Figure 6, the radiation efficiency of the propose antenna is greater than 89% across the operation band. Simulation results shows that the antenna operates in the desired frequency bands with a suitable gain and radiation efficiency.

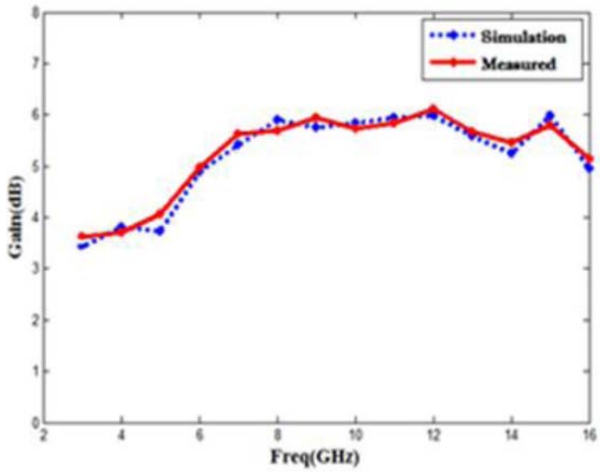


**Figure 5.** Measured and simulated gains of the antenna.

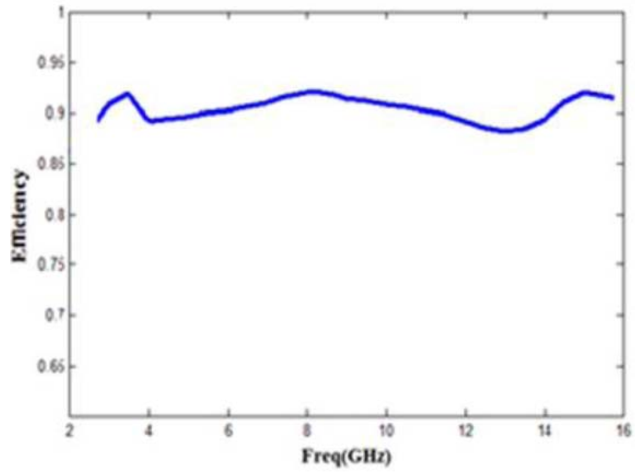


**Figure 6.** Radiation efficiency of the antenna.

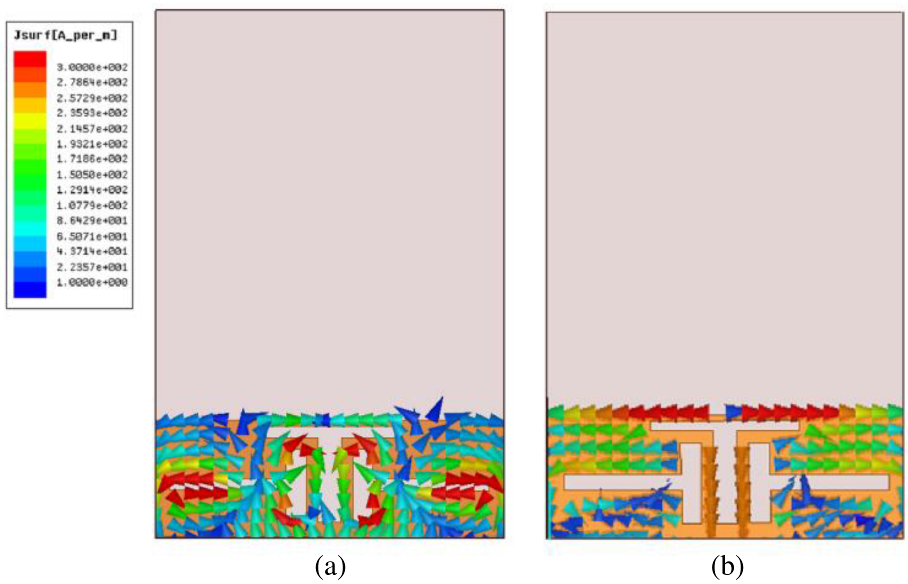


**Figure 7.** Current distributions in the ground plane for proposed antenna at the additional resonances frequencies, (a) 12.1 GHz, (b) 15.3 GHz.

Figures 7(a) and (b) show the current distributions at the resonance frequencies of 12.1 and 15.3 GHz on the proposed antenna. Figure 7(a) shows that the current distribution is strong around the pair of rotated T-shaped slots, which results in adding resonance properties at 12.1 GHz. Also Figure 7(b) shows that the current distribution is strong around the pairs of T-shaped slots at 15.3 GHz.

Figure 8 shows the measured radiation patterns of the fabricated antenna, obtained for the $y$-$z$ plane ($E$-plane) and the $x$-$z$ plane ($H$-plane) at 4.5, 10 and 13.5 GHz. It can be seen that the patterns in the $H$-plane are omnidirectional as expected, whereas in the $E$-plane, radiation patterns have a dumbbell shape. The cross-polarization levels are generally much lower than the co-polarization ones and on the $E$-plane stay at relatively low levels over the whole operating frequency band. Note that the fabricated antenna actually radiates over a wide frequency band.

In order to characterize the radiating properties of the proposed antenna in the in-body microwave imagine applications, it is necessary to test the proposed antenna in the vicinity of the human body tissues. The human body model constituent materials are dry skin and breast tissues [Figure 9]. The

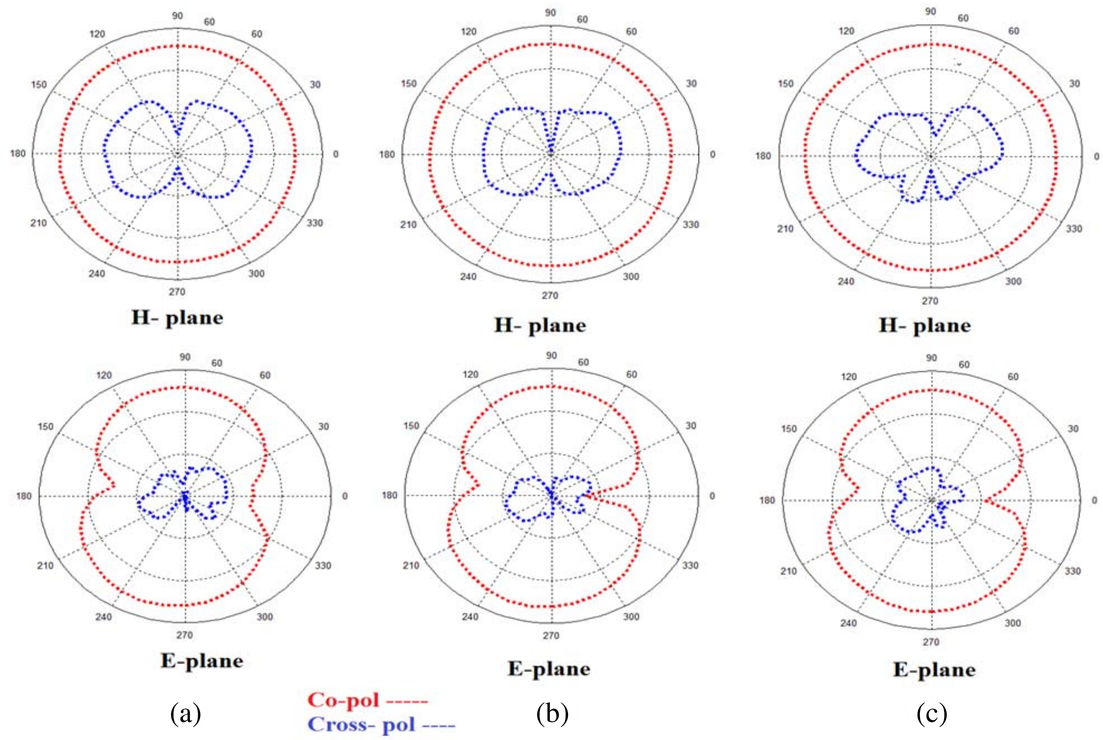


**Figure 8.** Measured radiation patterns of the proposed antenna, (a) 4.5 GHz, (b) 10 GHz, and (c) 13.5 GHz.

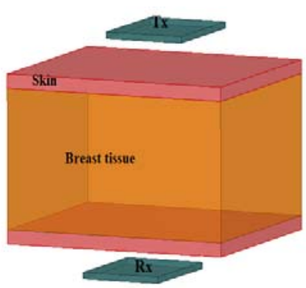


| | Skindry | Breast |
|---|---|---|
| Conductivity[S/m] | 7.45 | 0.71 |
| permittivity | 31.77 | 3.94 |
| Loss tangent | 0.44 | 0.34 |

**Figure 9.** Configuration of the compressed breast model with two antennas.

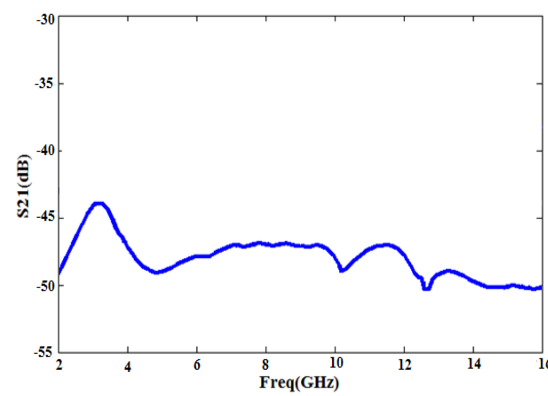


**Figure 10.** The transmission parameter $S_{21}$ of the antenna.

electromagnetic properties of the two layers including relative permittivity, conductivity and loss tangent at 9.5 GHz are given in [26]. The size of the human body model is 90 mm $*$ 90 mm $*$ 45 mm with the skin layer of the same size with thickness 2 mm on the top and bottom of it.

Note that the computer used for these simulations has 64 GB RAM, and these simulations have been done in the antenna and microwave laboratory in the Department of Electrical Engineering, Shahid Beheshti University G.C (SBU), Tehran, Iran. The transmission properties of the proposed monopole antenna have been investigated. In order to evaluate the transmission characteristics of the proposed UWB antenna, face-to-face orientation in close proximity of the human body model was chosen. In this case, two identical prototypes of the proposed monopole antenna have been placed on two different sides of the human body model, as shown in Figure 9. The transmission parameter $S_{21}$ is plotted in Figure 10. It is seen that the $S_{21}$ of the proposed monopole antenna exhibits approximately flat magnitude of transfer gain in the bandwidth of the proposed antenna.

### 3.2. The Time-Domain Behavior

To examine the antenna performance in time domain, the magnitude of the transfer between the pair of identical antennas, one for transmitting (Tx) and one for receiving (Rx), is simulated. The transfer function is transformed to the time domain by applying the Inverse Fourier Transform. The received signal can be obtained by convolving the input pulse with impulse response of the antenna system.

The proposed antennas are assumed to be excited by the UWB signal to examine the time domain response of the proposed antenna. In the simulation, the antenna pair, aligned face to face and side by side with a distance 40 cm, was placed. A Gaussian signal with bandwidth of (2.96–15.8) GHz shown in Figure 11(a) is applied at the input of the transmitting antenna. It can be seen from Figure 11 that the received signal has a less distortion and is very similar to transmitted signal.

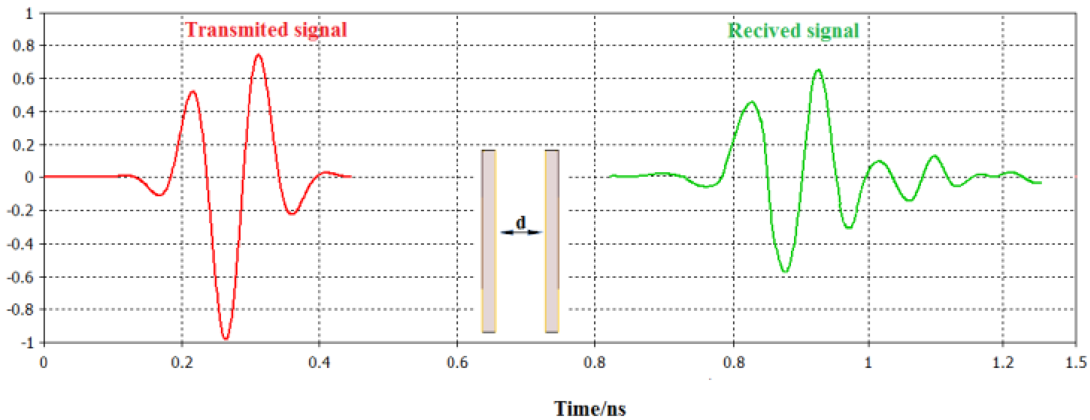


(a)

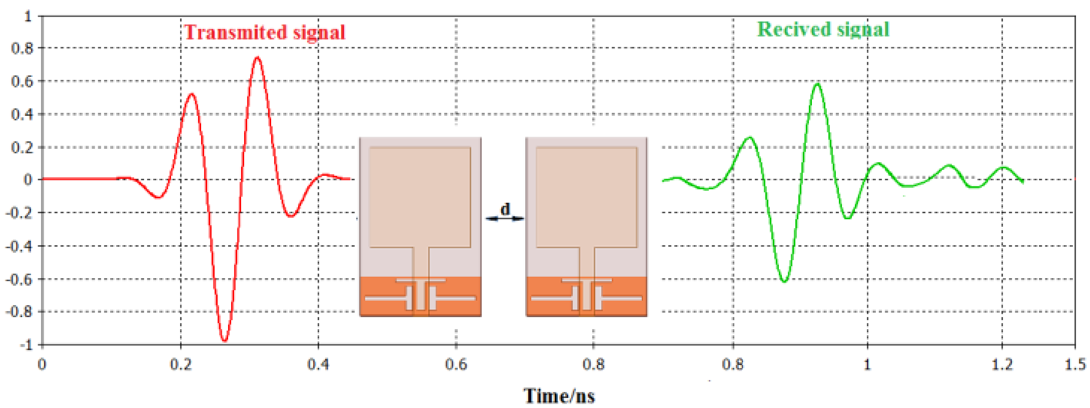


(b)

**Figure 11.** Transmitted and received signals, (a) face to face and (b) side by side.

## 4. CONCLUSION

In this paper, a planar monopole antenna with bandwidth enhancement is proposed for UWB-based breast imaging application. In order to enhance bandwidth, we use a pair of rotated T-shaped slots and another T-shaped slot that placed in between the two slots in the ground plane, hence much wider impedance bandwidth was produced. Simulated and measured results show that the presented optimized antenna has good frequency domain behavior, showing good matching, transmission and time domain behavior. Results show that the antenna operates in the desired frequency bands with a suitable gain and radiation efficiency. The proposed monopole antenna can be a good candidate for circular cylindrical microwave imaging system applications.

## REFERENCES


1. Balasubramanian, V. and A. Stranieri, "Performance evaluation of the dependable properties of a body area wireless sensor network," *International Conference on Optimization, Reliability, and Information Technology (ICROIT)*, 229–234, 2014.
2. Lee, C., J. Kim, H. S. Lee, and J. Kim, "Physical layer designs for WBAN systems in IEEE 802.15.6 proposals," *9th International Symposium on Communications and Information Technology, ISCIT 2009*, 841–844, 2009.
3. Malik, B. and V. R. Singh, "A survey of research in WBAN for biomedical and scientific applications," *Health and Technology*, Vol. 3, 227–235, 2013.
4. Otto, C. A., E. Jovanov, and A. Milenkovic, "A WBAN-based system for health monitoring at home," *3rd IEEE/EMBS International Summer School on Medical Devices and Biosensors*, 20–23, 2006.
5. Shahzad, A., M. O'Halloran, E. Jones, and M. Glavin, "A preprocessing filter for multistatic microwave breast imaging for enhanced tumour detection," *Progress In Electromagnetics Research B*, Vol. 57, 115–126, 2014.
6. Zhang, H., T. Arslan, and B. Flynn, "A single antenna based microwave system for breast cancer detection: Experimental results," *Loughborough Antennas and Propagation Conference (LAPC)*, 477–481, 2013.
7. Ireland, D., K. Bialkowski, and A. Abbosh, "Microwave imaging for brain stroke detection using born iterative method," *IET Microwaves, Antennas & Propagation*, Vol. 7, 909–915, 2013.
8. Zasowski, T., G. Meyer, F. Althaus, and A. Wittneben, "UWB signal propagation at the human head," *IEEE Transactions on Microwave Theory and Techniques*, Vol. 54, 1836–1845, 2006.
9. Huo, Y., R. Bansal, and Q. Zhu, "Breast tumor characterization via complex natural resonances," *IEEE MTT-S International Microwave Symposium Digest*, 387–390, 2003.
10. Huynh, P. T., A. M. Jarolimek, and S. Daye, "The false-negative mammogram," *Radiographics*, Vol. 18, 1137–1154, 1998.
11. Pancera, E. and W. Wiesbeck, "Fidelity based optimization of UWB antenna-radiation for medical applications," *2011 IEEE International Symposium on Antennas and Propagation (APSURSI)*, 2411–2414, 2011.
12. Bond, E. J., X. Li, S. C. Hagness, and B. D. van Veen, "Microwave imaging via space-time beamforming for early detection of breast cancer," *IEEE Transactions on Antennas and Propagation*, Vol. 51, 1690–1705, 2003.
13. Meaney, P. M., K. D. Paulsen, J. T. Chang, M. W. Fanning, and A. Hartov, "Nonactive antenna compensation for fixed-array microwave imaging. II. Imaging results," *IEEE Transactions on Medical Imaging*, Vol. 18, 508–518, 1999.
14. Khor, W. C., M. E. Bialkowski, A. Abbosh, N. Seman, and S. Crozier, "An ultra wideband microwave imaging system for breast cancer detection," *IEICE Transactions on Communications*, Vol. 90, 2376–2381, 2007.
15. Mohammed, B. A. J., A. M. Abbosh, and P. Sharpe, "Planar array of corrugated tapered slot antennas for ultrawideband biomedical microwave imaging system," *International Journal of RF and Microwave Computer-Aided Engineering*, Vol. 23, 59–66, 2013.
16. Bourqui, J., M. Okoniewski, and E. C. Fear, "Balanced antipodal Vivaldi antenna with dielectric director for near-field microwave imaging," *IEEE Transactions on Antennas and Propagation*, Vol. 58, 2318–2326, 2010.
17. Hossain, I., S. Noghanian, and S. Pistorius, "A diamond shaped small planar ultra wide band (UWB) antenna for microwave imaging purpose," *IEEE Antennas and Propagation Society International Symposium*, 5713–5716, 2007.
18. Li, X., M. Jalivand, Y. Sit, and T. Zwick, "A compact double-layer on-body matched bowtie antenna for medical diagnostics," *IEEE Transactions on Antennas and Propagation*, 1808–1816, 2014.

19. Shannon, C. J., E. C. Fear, and M. Okoniewski, "Dielectric-filled slotline bowtie antenna for breast cancer detection," *Electronics Letters*, Vol. 41, 388–390, 2005.
20. Nilavalan, R., I. J. Craddock, A. Preece, J. Leendertz, and R. Benjamin, "Wideband microstrip patch antenna design for breast cancer tumour detection," *IET Microwaves, Antennas & Propagation*, Vol. 1, 277–281, 2007.
21. Kumar, G. and K. P. Ray, *Broadband Microstrip Antennas*, Artech House, 2002.
22. http://www.emtalk.com/mscalc.php.
23. Ansoft High Frequency Structure Simulation (HFSS), Ver. 13, Ansoft Corporation, 2010.
24. Computer Simulation Technology (CST) Microwave Studio Software, Version 5.0.
25. Foudazi, A., H. R. Hassani, and S. M. A. Nezhad, "Small UWB planar monopole antenna with added GPS/GSM/WLAN bands," *IEEE Transactions on Antennas and Propagation*, Vol. 60, 2987–2992, 2012.
26. http://niremf.ifac.cnr.it/tissprop/htmlclie/htmlclie.htm.